

Limits on anomalous triple gauge couplings in $p\bar{p}$ collisions at $\sqrt{s} = 1.96$ TeV

T. Aaltonen,²³ A. Abulencia,²⁴ J. Adelman,¹³ T. Affolder,¹⁰ T. Akimoto,⁵⁵ M. G. Albrow,¹⁷ S. Amerio,⁴³ D. Amidei,³⁵ A. Anastassov,⁵² K. Anikeev,¹⁷ A. Annovi,¹⁹ J. Antos,¹⁴ M. Aoki,⁵⁵ G. Apollinari,¹⁷ T. Arisawa,⁵⁷ A. Artikov,¹⁵ W. Ashmanskas,¹⁷ A. Attal,³ A. Aurisano,⁵³ F. Azfar,⁴² P. Azzi-Bacchetta,⁴³ P. Azzurri,⁴⁶ N. Bacchetta,⁴³ W. Badgett,¹⁷ A. Barbaro-Galtieri,²⁹ V. E. Barnes,⁴⁸ B. A. Barnett,²⁵ S. Baroiant,⁷ V. Bartsch,³¹ G. Bauer,³³ P.-H. Beauchemin,³⁴ F. Bedeschi,⁴⁶ S. Behari,²⁵ G. Bellettini,⁴⁶ J. Bellinger,⁵⁹ A. Belloni,³³ D. Benjamin,¹⁶ A. Beretvas,¹⁷ J. Beringer,²⁹ T. Berry,³⁰ A. Bhatti,⁵⁰ M. Binkley,¹⁷ D. Bisello,⁴³ I. Bizjak,³¹ R. E. Blair,² C. Blocker,⁶ B. Blumenfeld,²⁵ A. Bocci,¹⁶ A. Bodek,⁴⁹ V. Boisvert,⁴⁹ G. Bolla,⁴⁸ A. Bolshov,³³ D. Bortoletto,⁴⁸ J. Boudreau,⁴⁷ A. Boveia,¹⁰ B. Brau,¹⁰ L. Brigliadori,⁵ C. Bromberg,³⁶ E. Brubaker,¹³ J. Budagov,¹⁵ H. S. Budd,⁴⁹ S. Budd,²⁴ K. Burkett,¹⁷ G. Busetto,⁴³ P. Bussey,²¹ A. Buzatu,³⁴ K. L. Byrum,² S. Cabrera,^{16,q} M. Campanelli,²⁰ M. Campbell,³⁵ F. Canelli,¹⁷ A. Canepa,⁴⁵ S. Carillo,^{18,j} D. Carlsmith,⁵⁹ R. Carosi,⁴⁶ S. Carron,³⁴ B. Casal,¹¹ M. Casarsa,⁵⁴ A. Castro,⁵ P. Catastini,⁴⁶ D. Cauz,⁵⁴ M. Cavalli-Sforza,³ A. Cerri,²⁹ L. Cerrito,^{31,n} S. H. Chang,²⁸ Y. C. Chen,¹ M. Chertok,⁷ G. Chiarelli,⁴⁶ G. Chlachidze,¹⁷ F. Chlebana,¹⁷ I. Cho,²⁸ K. Cho,²⁸ D. Chokheli,¹⁵ J. P. Chou,²² G. Choudalakis,³³ S. H. Chuang,⁵² K. Chung,¹² W. H. Chung,⁵⁹ Y. S. Chung,⁴⁹ M. Cilijak,⁴⁶ C. I. Ciobanu,²⁴ M. A. Ciocci,⁴⁶ A. Clark,²⁰ D. Clark,⁶ M. Coca,¹⁶ G. Compostella,⁴³ M. E. Convery,⁵⁰ J. Conway,⁷ B. Cooper,³¹ K. Copic,³⁵ M. Cordelli,¹⁹ G. Cortiana,⁴³ F. Crescioli,⁴⁶ C. Cuenca Almenar,^{7,r} J. Cuevas,^{11,m} R. Culbertson,¹⁷ J. C. Cully,³⁵ S. DaRonco,⁴³ M. Datta,¹⁷ S. D'Auria,²¹ T. Davies,²¹ D. Dagenhart,¹⁷ P. de Barbaro,⁴⁹ S. De Cecco,⁵¹ A. Deisher,²⁹ G. De Lentdecker,^{49,d} G. De Lorenzo,³ M. Dell'Orso,⁴⁶ F. Delli Paoli,⁴³ L. Demortier,⁵⁰ J. Deng,¹⁶ M. Deninno,⁵ D. De Pedis,⁵¹ P. F. Derwent,¹⁷ G. P. Di Giovanni,⁴⁴ C. Dionisi,⁵¹ B. Di Ruzza,⁵⁴ J. R. Dittmann,⁴ M. D'Onofrio,³ C. Dörr,²⁶ S. Donati,⁴⁶ P. Dong,⁸ J. Donini,⁴³ T. Dorigo,⁴³ S. Dube,⁵² J. Efron,³⁹ R. Erbacher,⁷ D. Errede,²⁴ S. Errede,²⁴ R. Eusebi,¹⁷ H. C. Fang,²⁹ S. Farrington,³⁰ I. Fedorko,⁴⁶ W. T. Fedorko,¹³ R. G. Feild,⁶⁰ M. Feindt,²⁶ J. P. Fernandez,³² R. Field,¹⁸ G. Flanagan,⁴⁸ R. Forrest,⁷ S. Forrester,⁷ M. Franklin,²² J. C. Freeman,²⁹ I. Furic,¹³ M. Gallinaro,⁵⁰ J. Galyardt,¹² J. E. Garcia,⁴⁶ F. Garberon,¹⁰ A. F. Garfinkel,⁴⁸ C. Gay,⁶⁰ H. Gerberich,²⁴ D. Gerdes,³⁵ S. Giagu,⁵¹ P. Giannetti,⁴⁶ K. Gibson,⁴⁷ J. L. Gimmell,⁴⁹ C. Ginsburg,¹⁷ N. Giokaris,^{15,b} M. Giordani,⁵⁴ P. Giromini,¹⁹ M. Giunta,⁴⁶ G. Giurgiu,²⁵ V. Glagolev,¹⁵ D. Glenzinski,¹⁷ M. Gold,³⁷ N. Goldschmidt,¹⁸ J. Goldstein,^{42,c} A. Golossanov,¹⁷ G. Gomez,¹¹ G. Gomez-Ceballos,³³ M. Goncharov,⁵³ O. González,³² I. Gorelov,³⁷ A. T. Goshaw,¹⁶ K. Goulianos,⁵⁰ A. Gresele,⁴³ S. Grinstein,²² C. Grosso-Pilcher,¹³ R. C. Group,¹⁷ U. Grundler,²⁴ J. Guimaraes da Costa,²² Z. Gunay-Unalan,³⁶ C. Haber,²⁹ K. Hahn,³³ S. R. Hahn,¹⁷ E. Halkiadakis,⁵² A. Hamilton,²⁰ B.-Y. Han,⁴⁹ J. Y. Han,⁴⁹ R. Handler,⁵⁹ F. Happacher,¹⁹ K. Hara,⁵⁵ D. Hare,⁵² M. Hare,⁵⁶ S. Harper,⁴² R. F. Harr,⁵⁸ R. M. Harris,¹⁷ M. Hartz,⁴⁷ K. Hatakeyama,⁵⁰ J. Hauser,⁸ C. Hays,⁴² M. Heck,²⁶ A. Heijboer,⁴⁵ B. Heinemann,²⁹ J. Heinrich,⁴⁵ C. Henderson,³³ M. Herndon,⁵⁹ J. Heuser,²⁶ D. Hidas,¹⁶ C. S. Hill,^{10,c} D. Hirschbuehl,²⁶ A. Hocker,¹⁷ A. Holloway,²² S. Hou,¹ M. Houlden,³⁰ S.-C. Hsu,⁹ B. T. Huffman,⁴² R. E. Hughes,³⁹ U. Husemann,⁶⁰ J. Huston,³⁶ J. Incandela,¹⁰ G. Introzzi,⁴⁶ M. Iori,⁵¹ A. Ivanov,⁷ B. Iyutin,³³ E. James,¹⁷ D. Jang,⁵² B. Jayatilaka,¹⁶ D. Jeans,⁵¹ E. J. Jeon,²⁸ S. Jindariani,¹⁸ W. Johnson,⁷ M. Jones,⁴⁸ K. K. Joo,²⁸ S. Y. Jun,¹² J. E. Jung,²⁸ T. R. Junk,²⁴ T. Kamon,⁵³ P. E. Karchin,⁵⁸ Y. Kato,⁴¹ Y. Kemp,²⁶ R. Kephart,¹⁷ U. Kerzel,²⁶ V. Khotilovich,⁵³ B. Kilminster,³⁹ D. H. Kim,²⁸ H. S. Kim,²⁸ J. E. Kim,²⁸ M. J. Kim,¹⁷ S. B. Kim,²⁸ S. H. Kim,⁵⁵ Y. K. Kim,¹³ N. Kimura,⁵⁵ L. Kirsch,⁶ S. Klimenko,¹⁸ M. Klute,³³ B. Knuteson,³³ B. R. Ko,¹⁶ K. Kondo,⁵⁷ D. J. Kong,²⁸ J. Konigsberg,¹⁸ A. Korytov,¹⁸ A. V. Kotwal,¹⁶ A. C. Kraan,⁴⁵ J. Kraus,²⁴ M. Kreps,²⁶ J. Kroll,⁴⁵ N. Krumnack,⁴ M. Kruse,¹⁶ V. Krutelyov,¹⁰ T. Kubo,⁵⁵ S. E. Kuhlmann,² T. Kuhr,²⁶ N. P. Kulkarni,⁵⁸ Y. Kusakabe,⁵⁷ S. Kwang,¹³ A. T. Laasanen,⁴⁸ S. Lai,³⁴ S. Lami,⁴⁶ S. Lammel,¹⁷ M. Lancaster,³¹ R. L. Lander,⁷ K. Lannon,³⁹ A. Lath,⁵² G. Latino,⁴⁶ I. Lazzizzera,⁴³ T. LeCompte,² J. Lee,⁴⁹ J. Lee,²⁸ Y. J. Lee,²⁸ S. W. Lee,^{53,p} R. Lefèvre,²⁰ N. Leonardo,³³ S. Leone,⁴⁶ S. Levy,¹³ J. D. Lewis,¹⁷ C. Lin,⁶⁰ C. S. Lin,¹⁷ M. Lindgren,¹⁷ E. Lipeles,⁹ A. Lister,⁷ D. O. Litvintsev,¹⁷ T. Liu,¹⁷ N. S. Lockyer,⁴⁵ A. Loginov,⁶⁰ M. Loretì,⁴³ R.-S. Lu,¹ D. Lucchesi,⁴³ P. Lujan,²⁹ P. Lukens,¹⁷ G. Lungu,¹⁸ L. Lyons,⁴² J. Lys,²⁹ R. Lysak,¹⁴ E. Lytken,⁴⁸ P. Mack,²⁶ D. MacQueen,³⁴ R. Madrak,¹⁷ K. Maeshima,¹⁷ K. Makhoul,³³ T. Maki,²³ P. Maksimovic,²⁵ S. Malde,⁴² S. Malik,³¹ G. Manca,³⁰ A. Manousakis,^{15,b} F. Margaroli,⁵ R. Marginean,¹⁷ C. Marino,²⁶ C. P. Marino,²⁴ A. Martin,⁶⁰ M. Martin,²⁵ V. Martin,^{21,h} M. Martínez,³ R. Martínez-Ballarín,³² T. Maruyama,⁵⁵ P. Mastrandrea,⁵¹ T. Masubuchi,⁵⁵ H. Matsunaga,⁵⁵ M. E. Mattson,⁵⁸ R. Mazini,³⁴ P. Mazzanti,⁵ K. S. McFarland,⁴⁹ P. McIntyre,⁵³ R. McNulty,^{30,g} A. Mehta,³⁰ P. Mehtala,²³ S. Menzemer,^{11,i} A. Menzione,⁴⁶ P. Merkel,⁴⁸ C. Mesropian,⁵⁰ A. Messina,³⁶ T. Miao,¹⁷ N. Miladinovic,⁶ J. Miles,³³ R. Miller,³⁶ C. Mills,¹⁰ M. Milnik,²⁶ A. Mitra,¹ G. Mitselmakher,¹⁸ A. Miyamoto,²⁷ S. Moed,²⁰ N. Moggi,⁵ B. Mohr,⁸ C. S. Moon,²⁸ R. Moore,¹⁷ M. Morello,⁴⁶ P. Movilla Fernandez,²⁹ J. Mülmenstädt,²⁹ A. Mukherjee,¹⁷ Th. Müller,²⁶ R. Mumford,²⁵ P. Murat,¹⁷ M. Mussini,⁵ J. Nachtman,¹⁷ A. Nagano,⁵⁵ J. Naganoma,⁵⁷ K. Nakamura,⁵⁵ I. Nakano,⁴⁰

A. Napier,⁵⁶ V. Necula,¹⁶ C. Neu,⁴⁵ M. S. Neubauer,⁹ J. Nielsen,^{29,o} L. Nodulman,² O. Normiella,³ E. Nurse,³¹ S. H. Oh,¹⁶ Y. D. Oh,²⁸ I. Oksuzian,¹⁸ T. Okusawa,⁴¹ R. Oldeman,³⁰ R. Orava,²³ K. Osterberg,²³ C. Pagliarone,⁴⁶ E. Palencia,¹¹ V. Papadimitriou,¹⁷ A. Papaikonomou,²⁶ A. A. Paramonov,¹³ B. Parks,³⁹ S. Pashapour,³⁴ J. Patrick,¹⁷ G. Pauletta,⁵⁴ M. Paulini,¹² C. Paus,³³ D. E. Pellett,⁷ A. Penzo,⁵⁴ T. J. Phillips,¹⁶ G. Piacentino,⁴⁶ J. Piedra,⁴⁴ L. Pinera,¹⁸ K. Pitts,²⁴ C. Plager,⁸ L. Pondrom,⁵⁹ X. Portell,³ O. Poukhov,¹⁵ N. Pounder,⁴² F. Prakoshyn,¹⁵ A. Pronko,¹⁷ J. Proudfoot,² F. Ptohos,^{19,f} G. Punzi,⁴⁶ J. Pursley,²⁵ J. Rademacker,^{42,c} A. Rahaman,⁴⁷ V. Ramakrishnan,⁵⁹ N. Ranjan,⁴⁸ I. Redondo,³² B. Reisert,¹⁷ V. Rekovic,³⁷ P. Renton,⁴² M. Rescigno,⁵¹ S. Richter,²⁶ F. Rimondi,⁵ L. Ristori,⁴⁶ A. Robson,²¹ T. Rodrigo,¹¹ E. Rogers,²⁴ S. Rolli,⁵⁶ R. Roser,¹⁷ M. Rossi,⁵⁴ R. Rossin,¹⁰ P. Roy,³⁴ A. Ruiz,¹¹ J. Russ,¹² V. Rusu,¹³ H. Saarikko,²³ A. Safonov,⁵³ W. K. Sakumoto,⁴⁹ G. Salamanna,⁵¹ O. Saltó,³ L. Santi,⁵⁴ S. Sarkar,⁵¹ L. Sartori,⁴⁶ K. Sato,¹⁷ P. Savard,³⁴ A. Savoy-Navarro,⁴⁴ T. Scheidle,²⁶ P. Schlabach,¹⁷ E. E. Schmidt,¹⁷ M. P. Schmidt,⁶⁰ M. Schmitt,³⁸ T. Schwarz,⁷ L. Scodellaro,¹¹ A. L. Scott,¹⁰ A. Scribano,⁴⁶ F. Scuri,⁴⁶ A. Sedov,⁴⁸ S. Seidel,³⁷ Y. Seiya,⁴¹ A. Semenov,¹⁵ L. Sexton-Kennedy,¹⁷ A. Sfyrla,²⁰ S. Z. Shalhout,⁵⁸ M. D. Shapiro,²⁹ T. Shears,³⁰ P. F. Shepard,⁴⁷ D. Sherman,²² M. Shimojima,^{55,l} M. Shochet,¹³ Y. Shon,⁵⁹ I. Shreyber,²⁰ A. Sidoti,⁴⁶ P. Sinervo,³⁴ A. Sisakyan,¹⁵ J. Sjolin,⁴² A. J. Slaughter,¹⁷ J. Slaunwhite,³⁹ K. Sliwa,⁵⁶ J. R. Smith,⁷ F. D. Snider,¹⁷ R. Snihur,³⁴ M. Soderberg,³⁵ A. Soha,⁷ S. Somalwar,⁵² V. Sorin,³⁶ J. Spalding,¹⁷ F. Spinella,⁴⁶ T. Spreitzer,³⁴ P. Squillacioti,⁴⁶ M. Stanitzki,⁶⁰ A. Staveris-Polykalas,⁴⁶ R. St. Denis,²¹ B. Stelzer,⁸ O. Stelzer-Chilton,⁴² D. Stentz,³⁸ J. Strologas,³⁷ D. Stuart,¹⁰ J. S. Suh,²⁸ A. Sukhanov,¹⁸ H. Sun,⁵⁶ I. Suslov,¹⁵ T. Suzuki,⁵⁵ A. Taffard,^{24,q} R. Takashima,⁴⁰ Y. Takeuchi,⁵⁵ R. Tanaka,⁴⁰ M. Tecchio,³⁵ P. K. Teng,¹ K. Terashi,⁵⁰ J. Thom,^{17,e} A. S. Thompson,²¹ E. Thomson,⁴⁵ P. Tipton,⁶⁰ V. Tiwari,¹² S. Tkaczyk,¹⁷ D. Toback,⁵³ S. Tokar,¹⁴ K. Tollefson,³⁶ T. Tomura,⁵⁵ D. Tonelli,⁴⁶ S. Torre,¹⁹ D. Torretta,¹⁷ S. Tourneur,⁴⁴ W. Trischuk,³⁴ S. Tsuno,⁴⁰ Y. Tu,⁴⁵ N. Turini,⁴⁶ F. Ukegawa,⁵⁵ S. Uozumi,⁵⁵ S. Vallecorsa,²⁰ N. van Remortel,²³ A. Varganov,³⁵ E. Vataga,³⁷ F. Vazquez,^{18,j} G. Velev,¹⁷ C. Vellidis,^{46,b} G. Veramendi,²⁴ V. Veszpremi,⁴⁸ M. Vidal,³² R. Vidal,¹⁷ I. Vila,¹¹ R. Vilar,¹¹ T. Vine,³¹ M. Vogel,³⁷ I. Vollrath,³⁴ I. Volobouev,^{29,p} G. Volpi,⁴⁶ F. Würthwein,⁹ P. Wagner,⁵³ R. G. Wagner,² R. L. Wagner,¹⁷ J. Wagner,²⁶ W. Wagner,²⁶ R. Wallny,⁸ S. M. Wang,¹ A. Warburton,³⁴ D. Waters,³¹ M. Weinberger,⁵³ W. C. Wester III,¹⁷ B. Whitehouse,⁵⁶ D. Whiteson,^{45,q} A. B. Wicklund,² E. Wicklund,¹⁷ G. Williams,³⁴ H. H. Williams,⁴⁵ P. Wilson,¹⁷ B. L. Winer,³⁹ P. Wittich,^{17,e} S. Wolbers,¹⁷ C. Wolfe,¹³ T. Wright,³⁵ X. Wu,²⁸ S. M. Wynne,³⁰ A. Yagil,⁹ K. Yamamoto,⁴¹ J. Yamaoka,⁵² T. Yamashita,⁴⁰ C. Yang,⁶⁰ U. K. Yang,^{13,k} Y. C. Yang,²⁸ W. M. Yao,²⁹ G. P. Yeh,¹⁷ J. Yoh,¹⁷ K. Yorita,¹³ T. Yoshida,⁴¹ G. B. Yu,⁴⁹ I. Yu,²⁸ S. S. Yu,¹⁷ J. C. Yun,¹⁷ L. Zanello,⁵¹ A. Zanetti,⁵⁴ I. Zaw,²² X. Zhang,²⁴ J. Zhou,⁵² and S. Zucchelli⁵

(CDF Collaboration)^a¹*Institute of Physics, Academia Sinica, Taipei, Taiwan 11529, Republic of China*²*Argonne National Laboratory, Argonne, Illinois 60439, USA*³*Institut de Fisica d'Altes Energies, Universitat Autònoma de Barcelona, E-08193, Bellaterra (Barcelona), Spain*⁴*Baylor University, Waco, Texas 76798, USA*⁵*Istituto Nazionale di Fisica Nucleare, University of Bologna, I-40127 Bologna, Italy*⁶*Brandeis University, Waltham, Massachusetts 02254, USA*⁷*University of California, Davis, Davis, California 95616, USA*⁸*University of California, Los Angeles, Los Angeles, California 90024, USA*⁹*University of California, San Diego, La Jolla, California 92093, USA*¹⁰*University of California, Santa Barbara, Santa Barbara, California 93106, USA*¹¹*Instituto de Fisica de Cantabria, CSIC-University of Cantabria, 39005 Santander, Spain*¹²*Carnegie Mellon University, Pittsburgh, Pennsylvania 15213, USA*¹³*Enrico Fermi Institute, University of Chicago, Chicago, Illinois 60637, USA*¹⁴*Comenius University, 842 48 Bratislava, Slovakia; Institute of Experimental Physics, 040 01 Kosice, Slovakia*¹⁵*Joint Institute for Nuclear Research, RU-141980 Dubna, Russia*¹⁶*Duke University, Durham, North Carolina 27708, USA*¹⁷*Fermi National Accelerator Laboratory, Batavia, Illinois 60510, USA*¹⁸*University of Florida, Gainesville, Florida 32611, USA*¹⁹*Laboratori Nazionali di Frascati, Istituto Nazionale di Fisica Nucleare, I-00044 Frascati, Italy*²⁰*University of Geneva, CH-1211 Geneva 4, Switzerland*²¹*Glasgow University, Glasgow G12 8QQ, United Kingdom*²²*Harvard University, Cambridge, Massachusetts 02138, USA*²³*Division of High Energy Physics, Department of Physics, University of Helsinki, FIN-00014, Helsinki, Finland and Helsinki Institute of Physics, FIN-00014, Helsinki, Finland*

- ²⁴University of Illinois, Urbana, Illinois 61801, USA
- ²⁵The Johns Hopkins University, Baltimore, Maryland 21218, USA
- ²⁶Institut für Experimentelle Kernphysik, Universität Karlsruhe, 76128 Karlsruhe, Germany
- ²⁷High Energy Accelerator Research Organization (KEK), Tsukuba, Ibaraki 305, Japan
- ²⁸Center for High Energy Physics: Kyungpook National University, Taegu 702-701, Korea;
Seoul National University, Seoul 151-742, Korea;
SungKyunKwan University, Suwon 440-746, Korea
- ²⁹Ernest Orlando Lawrence Berkeley National Laboratory, Berkeley, California 94720, USA
- ³⁰University of Liverpool, Liverpool L69 7ZE, United Kingdom
- ³¹University College London, London WC1E 6BT, United Kingdom
- ³²Centro de Investigaciones Energeticas Medioambientales y Tecnologicas, E-28040 Madrid, Spain
- ³³Massachusetts Institute of Technology, Cambridge, Massachusetts 02139, USA
- ³⁴Institute of Particle Physics: McGill University, Montréal, Canada H3A 2T8
and University of Toronto, Toronto, Canada M5S 1A7
- ³⁵University of Michigan, Ann Arbor, Michigan 48109, USA
- ³⁶Michigan State University, East Lansing, Michigan 48824, USA
- ³⁷University of New Mexico, Albuquerque, New Mexico 87131, USA
- ³⁸Northwestern University, Evanston, Illinois 60208, USA
- ³⁹The Ohio State University, Columbus, Ohio 43210, USA
- ⁴⁰Okayama University, Okayama 700-8530, Japan
- ⁴¹Osaka City University, Osaka 588, Japan
- ⁴²University of Oxford, Oxford OX1 3RH, United Kingdom
- ⁴³University of Padova, Istituto Nazionale di Fisica Nucleare, Sezione di Padova-Trento, I-35131 Padova, Italy
- ⁴⁴LPNHE, Universite Pierre et Marie Curie/IN2P3-CNRS, UMR7585, Paris, F-75252 France
- ⁴⁵University of Pennsylvania, Philadelphia, Pennsylvania 19104, USA
- ⁴⁶Istituto Nazionale di Fisica Nucleare Pisa, Universities of Pisa, Siena
and Scuola Normale Superiore, I-56127 Pisa, Italy
- ⁴⁷University of Pittsburgh, Pittsburgh, Pennsylvania 15260, USA
- ⁴⁸Purdue University, West Lafayette, Indiana 47907, USA
- ⁴⁹University of Rochester, Rochester, New York 14627, USA
- ⁵⁰The Rockefeller University, New York, New York 10021, USA
- ⁵¹Istituto Nazionale di Fisica Nucleare, Sezione di Roma 1, University of Rome “La Sapienza”, I-00185 Roma, Italy
- ⁵²Rutgers University, Piscataway, New Jersey 08855, USA
- ⁵³Texas A&M University, College Station, Texas 77843, USA
- ⁵⁴Istituto Nazionale di Fisica Nucleare, University of Trieste/ Udine, Italy
- ⁵⁵University of Tsukuba, Tsukuba, Ibaraki 305, Japan
- ⁵⁶Tufts University, Medford, Massachusetts 02155, USA
- ⁵⁷Waseda University, Tokyo 169, Japan
- ⁵⁸Wayne State University, Detroit, Michigan 48201, USA

^aWith visitors as noted.

^bVisitor from University of Athens, 15784 Athens, Greece.

^cVisitor from University of Bristol, Bristol BS8 1TL, United Kingdom.

^dVisitor from University Libre de Bruxelles, B-1050 Brussels, Belgium.

^eVisitor from Cornell University, Ithaca, NY 14853, USA.

^fVisitor from University of Cyprus, Nicosia CY-1678, Cyprus.

^gVisitor from University College Dublin, Dublin 4, Ireland.

^hVisitor from University of Edinburgh, Edinburgh EH9 3JZ, United Kingdom.

ⁱVisitor from University of Heidelberg, D-69120 Heidelberg, Germany.

^jVisitor from Universidad Iberoamericana, Mexico D.F., Mexico.

^kVisitor from University of Manchester, Manchester M13 9PL, England.

^lVisitor from Nagasaki Institute of Applied Science, Nagasaki, Japan.

^mVisitor from University de Oviedo, E-33007 Oviedo, Spain.

ⁿVisitor from University of London, Queen Mary College, London, E1 4NS, England.

^oVisitor from University of California Santa Cruz, Santa Cruz, CA 95064, USA.

^pVisitor from Texas Tech University, Lubbock, TX 79409, USA.

^qVisitor from University of California Irvine, Irvine, CA 92697, USA.

^rVisitor from IFIC (CSIC-Universitat de Valencia), 46071 Valencia, Spain.

⁵⁹*University of Wisconsin, Madison, Wisconsin 53706, USA*⁶⁰*Yale University, New Haven, Connecticut 06520, USA*

(Received 17 May 2007; published 27 December 2007)

We present a search for anomalous triple gauge couplings (ATGC) in WW and WZ boson production. The boson pairs are produced in $p\bar{p}$ collisions at $\sqrt{s} = 1.96$ TeV, and the data sample corresponds to 350 pb^{-1} of integrated luminosity collected with the CDF II detector at the Fermilab Tevatron. In this search one W decays to leptons, and the other boson (W or Z) decays hadronically. Combining with a previously published CDF measurement of $W\gamma$ boson production yields ATGC limits of $-0.18 < \lambda < 0.17$ and $-0.46 < \Delta\kappa < 0.39$ at the 95% confidence level, using a cutoff scale $\Lambda = 1.5$ TeV.

DOI: [10.1103/PhysRevD.76.111103](https://doi.org/10.1103/PhysRevD.76.111103)

PACS numbers: 12.15.Ji, 13.40.Em, 14.70.Fm, 14.70.Hp

In the standard model (SM), the non-Abelian nature of the electroweak field theory predicts interactions between the massive gauge bosons. The resulting triple and quartic boson vertices and couplings are restricted by electroweak symmetry [1]. By experimentally measuring the strengths of these couplings we can test the SM and constrain possible deviations from it. One way to test a more general gauge interaction hypothesis is to formulate an effective theory and keep only the leading-order (LO) operators. This introduces two free parameters λ and $\Delta\kappa = \kappa - 1$ under the assumption of equal WWZ and $WW\gamma$ parameters [2], where $\lambda = \Delta\kappa = 0$ corresponds to the SM.

At the Fermilab Tevatron $p\bar{p}$ collider the anomalous triple gauge couplings (ATGC) contribution to the cross section for diboson production is a function of the parton center-of-mass energy $\sqrt{\hat{s}}$ and, in order to maintain unitarity in the model at high energies, a form factor

$$\lambda(\hat{s}) = \frac{\lambda}{(1 + \hat{s}/\Lambda^2)^2}, \quad \Delta\kappa(\hat{s}) = \frac{\Delta\kappa}{(1 + \hat{s}/\Lambda^2)^2}, \quad (1)$$

is introduced. We set the cutoff energy Λ to 1.5 TeV to preserve unitarity at the energies reached by the Tevatron [2]. The ATGC are enhanced at large scattering angles [2], making observables which are proportional to the gauge boson transverse momentum particularly effective.

In this paper, we present a search for ATGC in $p\bar{p}$ collisions using events in which a W decays to an electron or muon and its associated neutrino and the other boson (W or Z) decays hadronically. In what follows we refer to this event signature as $\ell\nu jj$. The search was performed with the signal region blinded until all selection criteria and background determinations were fixed. Since the detector dijet mass resolution does not permit separation of hadronic decays of Z and W bosons, we combine both WW and WZ in this analysis. The $\ell\nu jj$ channel has several good features: by identifying the p_T [3] of the ν with \cancel{E}_T , the $\ell\nu jj$ decay mode allows for a full reconstruction of the gauge boson transverse momentum; it utilizes the high branching fraction of W and Z into quarks; the leptonic decay of the boson gives a clear signature on which to trigger. However, due to the large W + jets background and the limited dijet mass resolution, no observation has yet been made of WW or WZ production in the $\ell\nu jj$ decay

mode at hadron colliders. In this analysis we measure the transverse momentum (p_T^W) distribution for $W \rightarrow \ell\nu$. The SM has strong cancellations between the s-channel and the u- or t-channel diagrams at high p_T^W , and any ATGC will tend to reduce the cancellations and substantially increase the cross section.

Previous limits on ATGC in the $\ell\nu jj$ channel in $p\bar{p}$ collisions at $\sqrt{s} = 1.8$ TeV have been reported by the CDF Collaboration, which obtained 95% confidence limits (C.L.) of $-1.11 < \lambda < 1.27$ and $-0.81 < \Delta\kappa < 0.84$ [4]. The D0 collaboration, using a larger data sample, reported 95% C.L. limits of $-0.36 < \lambda < 0.39$ and $-0.47 < \Delta\kappa < 0.63$ [5]. Results on ATGC have also been produced at LEP [6]. The LEP values are more precise, but the parameters fitted are not directly comparable as they are obtained at fixed \sqrt{s} values up to a maximum of 209 GeV, without the use of form factors of the type given in Eq. (1). For the Tevatron the spectrum in $\sqrt{\hat{s}}$ extends well beyond the reach of LEP, and these studies are potentially sensitive to the direct production of any new physics beyond the SM up to the kinematic limit.

The CDF II detector [7] is an approximately azimuthally and forward-backward symmetric apparatus centered on the $p\bar{p}$ interaction region and consists of a magnetic spectrometer surrounded by calorimeters and muon chambers. Charged tracks are detected using a 96-layer open-cell cylindrical drift chamber (COT) in a 1.4 T solenoidal magnetic field. Isolated high-momentum tracks are reconstructed in the COT with an efficiency close to 100% in the pseudorapidity region $|\eta| < 1$. Electromagnetic and hadronic calorimeters surround the tracking system. The calorimeters are segmented into projective geometry towers and cover the region $|\eta| < 3.6$. The central and forward electromagnetic calorimeters are lead-scintillator sampling devices, instrumented with proportional (central) and scintillating strip (forward) detectors that measure the position and transverse profile of electromagnetic showers at the position of the shower maximum. The hadron calorimeters are iron-scintillator sampling detectors. Muon drift chambers surround the calorimeters and, for this analysis, provide muon identification for $|\eta| < 1$. Gas Cherenkov counters in the region $3.7 < |\eta| < 4.7$ measure the average number of inelastic $p\bar{p}$ collisions per bunch crossing in order to compute the luminosity to an accuracy of 6% [8].

The trigger system selects events with a central ($|\eta| < 1$) electron candidate with $E_T > 18$ GeV or a muon candidate with $p_T > 18$ GeV/ c . Events reconstructed offline are required to contain an electron candidate with $E_T > 25$ GeV or a muon candidate with $p_T > 20$ GeV/ c , to ensure a trigger efficiency sufficiently constant in E_T and p_T . The trigger and lepton identification criteria are described in Ref. [9]. The data presented in this paper correspond to a total integrated luminosity of 350 ± 20 pb $^{-1}$ for the electron sample and 330 ± 20 pb $^{-1}$ for the muon sample.

Candidate events from W leptonic decays are selected by requiring the \cancel{E}_T , corrected for muons and jets, to be greater than 25 GeV. To further reduce the QCD multijet background, the W transverse mass is required to satisfy $m_T^W = \sqrt{2E_T\cancel{E}_T(1 - \cos\Delta\phi)} > 25$ GeV/ c^2 , where $\Delta\phi$ is the angle between the lepton candidate momentum vector and the \cancel{E}_T vector in the transverse plane. Events are required to have only one lepton candidate, no identified cosmic ray muon, and no identified photon conversion electron. Most $Z \rightarrow l^+l^-$ events that remain in the sample are rejected with a veto algorithm designed to identify event topologies consistent with a partially reconstructed second lepton [9].

The $\ell\nu jj$ event selection proceeds by requiring two or more jets. Jets are reconstructed using an iterative seed-based cone algorithm [10] that clusters energies measured in individual calorimeter towers. The jets are defined by the cone algorithm parameter $\Delta R = \sqrt{\Delta\phi^2 + \Delta\eta^2} \leq 0.4$. The measured jet E_T is corrected for calorimeter response and energy contributions from additional $p\bar{p}$ interactions in the same bunch crossing [11]. For this analysis, jets must have corrected $E_T > 20$ GeV and $|\eta| < 2$. To ensure that the event kinematics are well measured, events are rejected if any jet lies within $\Delta R = 0.5$ of the W decay lepton or another jet.

After event selection, 929 events in the electron channel and 688 events in the muon channel remain within the signal region. The signal region is defined as $56 < M_{jj} < 112$ GeV/ c^2 , where M_{jj} is the invariant mass of the two leading jets. Table I shows the expected and observed numbers of events, where the expected number of events takes account of kinematic and geometric acceptance, lepton identification efficiencies, and trigger efficiencies. The expected numbers of WW and WZ events are calculated using information from both data and Monte Carlo simulations. For the SM diboson production signals we use the PYTHIA Monte Carlo generator [12] and GEANT-based detector simulation [13] to predict the accepted event yields. The lepton efficiencies from these simulations are scaled to match the values measured from $Z \rightarrow l^+l^-$ events. The central muon efficiencies require a scale factor correction of 0.874 ± 0.009 . All other systems have scale factors close to unity. The expected event yields are based on the total signal cross sections of 12.4 ± 0.8 pb (WW)

TABLE I. Expected and observed data events for the $\ell\nu jj$ WW and WZ search in the signal region. The signal region is defined as $56 < M_{jj} < 112$ GeV/ c^2 . $e + \mu$ is a correlated estimation of both channels. The listed uncertainties are statistical and systematic combined.

	e	μ	$e + \mu$
WW	44.7 ± 7.6	34.4 ± 5.8	79.0 ± 13.4
WZ	6.7 ± 1.1	5.1 ± 0.9	11.8 ± 2.0
Signal	51.4 ± 8.7	39.5 ± 6.7	90.9 ± 15.5
$W + \text{jets}$	690.0 ± 52.0	552.2 ± 44.3	1242.2 ± 65.4
QCD Multijets	53.7 ± 21.5	11.9 ± 4.8	65.6 ± 26.2
$t\bar{t}$	30.9 ± 7.7	22.4 ± 5.6	53.3 ± 13.3
$Z + \text{jets}$	16.8 ± 3.4	26.9 ± 5.4	43.7 ± 8.7
$W(\tau\nu) + \text{jets}$	17.7 ± 3.5	21.9 ± 4.4	39.6 ± 7.9
Single	5.1 ± 1.3	3.6 ± 0.9	8.7 ± 2.2
Background	814.1 ± 57.0	639.0 ± 45.5	1453.1 ± 72.7
Expected	865.5 ± 57.7	678.5 ± 46.0	1544.0 ± 74.3
Observed	929	688	1617

and 4.0 ± 0.3 pb (WZ) from next-to-leading-order (NLO) predictions [14]. Sources of systematic uncertainty on the expected number of events include jet E_T corrections (11%), estimated from data events with two jets, $\gamma + \text{jet}$ events, and Monte Carlo simulations tuned to data [11]; higher-order QCD radiation estimated from variations of the initial and final state showering model (10%); NLO cross section normalization, taken from theory (7%); luminosity measurements (6%); and parton distribution functions (3%).

Backgrounds to WW and WZ production in the $\ell\nu jj$ event signature can be classified into three categories: electroweak (EWK), QCD multijets, and $W + \text{jets}$. EWK backgrounds contain real leptons from W and Z decays and include $W \rightarrow \tau\nu$, $Z \rightarrow l^+l^-$, top pair production and single top production. The QCD background arises from multijet events in which one jet is falsely identified as a lepton or contains a lepton not from W or Z decays, and which have mismeasured energy resulting in large \cancel{E}_T . The $W + \text{jets}$ background corresponds to production of single W bosons decaying to $e\nu$ or $\mu\nu$ accompanied by additional jets.

The EWK backgrounds are estimated from Monte Carlo simulations normalized to NLO predictions [15–17], using the same methods as for WW and WZ signal expectations.

The QCD background is estimated from data. Assuming no correlation between event \cancel{E}_T and energy in the vicinity of the lepton (lepton isolation energy), we extrapolate from sideband regions to predict the QCD content in the signal region, correcting for the EWK contributions [9]. By using several different ranges of lepton isolation energy and \cancel{E}_T we estimate a 40% QCD normalization uncertainty.

The $W + \text{jets}$ background is simulated using the ALPGEN Monte Carlo generator [18], followed by HERWIG [19] for the parton shower and fragmentation, and full GEANT

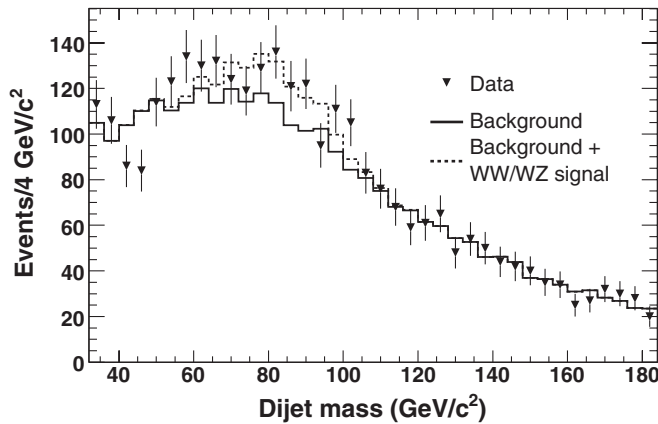


FIG. 1. Invariant mass reconstructed from the two jets with highest E_T . The measured data are fitted to the hypothesis of combined signal and background shapes.

detector simulation. The hard scattering process includes two partons in the final state. To further minimize the systematic uncertainties, we float the absolute $W + \text{jets}$ normalization in a fit to data (Fig. 1). In the fit, we allow for a linear dependence of the normalization on the dijet invariant mass (M_{jj}), derived from studies of the effect of renormalization scale variation. By normalizing $W + \text{jets}$ to the observed data, we achieve a normalization uncertainty of 5%. This should be contrasted with the 20% uncertainty on the NLO cross section that would otherwise have been used to normalize this contribution. The presence of ATGC contributions does not affect the $W + \text{jets}$ normalization. The reason for this is that any ATGC contribution is projected onto the fitted diboson signal shape. This factorization has been verified using ATGC Monte Carlo with very large coupling values.

Before probing the existence of ATGC, we test our sensitivity to SM WW and WZ production by fitting the dijet mass distribution to the background plus signal hypothesis in the extended dijet mass region $32 < M_{jj} < 184 \text{ GeV}/c^2$, using a lowered jet E_T threshold of 15 GeV. Previous measurements have put constraints on ATGC such that no significant contributions are expected to the inclusive diboson production. To verify if any such contributions are present is an important step for the internal consistency of the search. The result of the fit is $109 \pm 110(\text{stat}) \pm 54(\text{syst})$ $WW + WZ$ events, consistent with both the SM expectation of 160 events and also with no $WW + WZ$ production. We set a 95% C.L. upper limit of 36 pb on the combined $WW + WZ$ production cross section.

While we observe no significant evidence of SM $WW + WZ$ production, we can probe ATGC with the p_T^W distribution, for which we expect maximum sensitivity to ATGC. In particular, ATGC would result in an enhanced cross section at high p_T^W , where SM backgrounds are small. We perform a binned maximum likelihood fit to the measured p_T^W spectrum (Fig. 2), and observe no significant

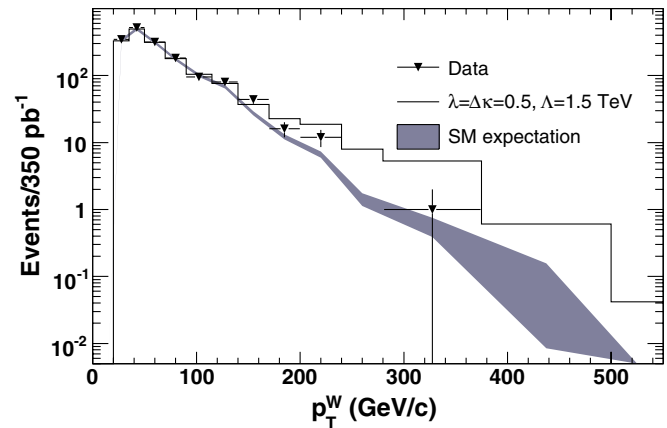


FIG. 2 (color online). p_T^W distribution used for setting the ATGC limits. Shown are the SM expectation, data points, and one ATGC scenario with $\lambda = \Delta\kappa = 0.5$ and $\Lambda = 1.5 \text{ TeV}$.

deviation from the SM. The ATGC signal is simulated at LO using the MCFM Monte Carlo generator [14] for the hard scatter process and fragmented with PYTHIA, followed by full GEANT detector simulation. A grid of points is simulated in the λ - $\Delta\kappa$ plane, and the expected numbers of events at each point are fitted to a quadratic form. We determine a two-dimensional 95% C.L. interval in λ and $\Delta\kappa$ corresponding to a change of 3.0 units in the logarithm of a binned likelihood combining all channels, relative to the maximum of the likelihood in λ and $\Delta\kappa$. Uncertainties from jet energy scale, renormalization scale, higher-order QCD radiation, parton distribution functions, and luminosity are included by a convolution of the likelihood with Gaussian-distributed systematic uncertainties. The dominant systematic uncertainty comes from the jet energy scale, whose correlations among bins, across channels, and between signal and background, are taken into account during the convolution process. The two-dimensional limits are shown in Fig. 3. We also present the one-

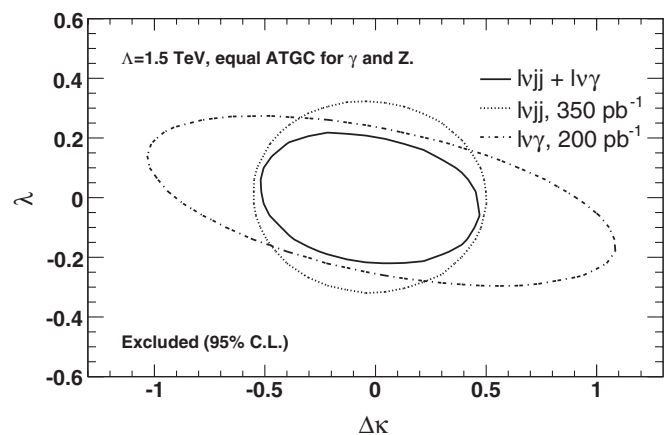


FIG. 3. Limits at 95% C.L. on ATGC using WW and WZ decays to $\ell\nu jj$, $W\gamma$ decays to $\ell\nu\gamma$, and the combination of both channels.

TABLE II. Allowed ATGC ranges for $\Lambda = 1.5$ TeV at 95% C.L., fixing the other coupling to the SM value.

	λ	$\Delta\kappa$
$\ell\nu jj$	(-0.28, 0.28)	(-0.50, 0.43)
$\ell\nu\gamma$ [20]	(-0.21, 0.19)	(-0.74, 0.73)
Combined	(-0.18, 0.17)	(-0.46, 0.39)

dimensional limits in Table II, where one of the anomalous couplings is held fixed to the SM value.

To increase our sensitivity to ATGC, we combine the $\ell\nu jj$ channel with a previously published CDF measurement of $W\gamma$ production in the $\ell\nu\gamma$ channel [20]. The $\ell\nu\gamma$ data set corresponds to about 200 pb⁻¹ of accumulated data. We use E_T of the γ to set limits using the same procedure as outlined above for the $\ell\nu jj$ channel, with the exception that the Baur Monte Carlo generator [21] is used for the ATGC signal. Systematic uncertainties for $\ell\nu\gamma$ that enter into the combination are signal acceptance (electrons 4.6%, muons 5%), signal and background NLO normalization (7%), luminosity (6%), and the rate of mis-measured photons due to jets. The rate of jets misreconstructed as photons is estimated from data and binned in E_T . The uncertainties on the electron and the muon channel acceptances are assumed to be correlated since they are both dominated by the photon identification uncertainty. The $\ell\nu\gamma$ and $\ell\nu jj$ channels are assumed to be uncorrelated except for the luminosity measurements. The derived $\ell\nu\gamma$ and combined limits are shown in Table II and Fig. 3. It can be seen that the $\ell\nu jj$ and $\ell\nu\gamma$ data have complementary sensitivity to $\Delta\kappa$ and λ .

In summary, we set limits on ATGC in 350 pb⁻¹ of $p\bar{p}$ collisions at $\sqrt{s} = 1.96$ TeV using the p_T^W from $\ell\nu jj$ WW and WZ decays. The couplings are restricted to $-0.28 < \lambda < 0.28$ and $-0.50 < \Delta\kappa < 0.43$, at 95% C.L. This restriction assumes a form factor cutoff $\Lambda = 1.5$ TeV and equal Z and γ couplings. The limits obtained in the $\ell\nu jj$ channel are improved by combining with previously published $W\gamma$ results, yielding the combined limits $-0.18 < \lambda < 0.17$ and $-0.46 < \Delta\kappa < 0.39$.

We thank the Fermilab staff and the technical staffs of the participating institutions for their vital contributions. This work was supported by the U.S. Department of Energy and National Science Foundation; the Italian Istituto Nazionale di Fisica Nucleare; the Ministry of Education, Culture, Sports, Science and Technology of Japan; the Natural Sciences and Engineering Research Council of Canada; the National Science Council of the Republic of China; the Swiss National Science Foundation; the A.P. Sloan Foundation; the Bundesministerium für Bildung und Forschung, Germany; the Korean Science and Engineering Foundation and the Korean Research Foundation; the Particle Physics and Astronomy Research Council and the Royal Society, UK; the Institut National de Physique Nucleaire et Physique des Particules/CNRS; the Russian Foundation for Basic Research; the Comisión Interministerial de Ciencia y Tecnología, Spain; the European Community's Human Potential Programme; the Slovak R&D Agency; and the Academy of Finland.

-
- [1] F. Mandl and G. Shaw, *Quantum Field Theory* (Wiley, New York, 1993).
- [2] K. Hagiwara *et al.*, Phys. Rev. D **41**, 2113 (1990).
- [3] We use a coordinate system where θ is the polar angle to the proton beam, ϕ is the azimuthal angle about the beam axis, and η is the pseudorapidity defined as $-\ln(\tan(\theta/2))$. The transverse momentum of a particle is denoted by $p_T \equiv p \sin\theta$. The analogous quantity defined using energies, $E_T \equiv E \sin\theta$, is called transverse energy. Missing transverse energy, \cancel{E}_T , is defined as the magnitude of $-\sum_i E_T^i \hat{n}_i$, where \hat{n}_i is a unit vector in the azimuthal plane that points from the collision vertex to the i th calorimeter tower.
- [4] F. Abe *et al.* (CDF Collaboration), Phys. Rev. Lett. **75**, 1017 (1995).
- [5] B. Abbott *et al.* (D0 Collaboration), Phys. Rev. D **62**, 052005 (2000).
- [6] P. Azzurri *et al.* (LEP Collaborations), CERN Report No. CERN-PH-EP-2006-042, 2006.
- [7] D. Acosta *et al.* (CDF Collaboration), Phys. Rev. D **71**, 032001 (2005); A. Abulencia *et al.* (CDF Collaboration), FERMILAB Report No. FERMILAB-PUB-05-360-E, 2005.
- [8] D. Acosta *et al.*, Nucl. Instrum. Methods Phys. Res., Sect. A **494**, 57 (2002).
- [9] D. Acosta *et al.* (CDF Collaboration), Phys. Rev. D **71**, 052003 (2005).
- [10] F. Abe *et al.* (CDF Collaboration), Phys. Rev. D **45**, 1448 (1992).
- [11] A. Bhatti *et al.*, Nucl. Instrum. Methods Phys. Res., Sect. A **566**, 375 (2006).
- [12] T. Sjöstrand *et al.*, Comput. Phys. Commun. **135**, 238 (2001); PYTHIA v6.216.
- [13] R. Brun and F. Carminati, CERN Program Library Long Writeup, W 5013, 1993 (unpublished), version 3.15.
- [14] J.M. Campbell and R.K. Ellis, Phys. Rev. D **60**, 113006 (1999).
- [15] Z. Sullivan, Phys. Rev. D **70**, 114012 (2004).
- [16] M. Cacciari *et al.*, J. High Energy Phys. **04** (2004) 068.

T. AALTONEN *et al.*

PHYSICAL REVIEW D **76**, 111103(R) (2007)

- [17] J. Campbell and R.K. Ellis, Phys. Rev. D **65**, 113007 (2002); MCFM v3.4.5.
- [18] M. L. Mangano *et al.*, J. High Energy Phys. 07 (2003) 001; ALPGEN v1.3.3.
- [19] G. Marchesini *et al.*, Comput. Phys. Commun. **67**, 465 (1992); G. Corcella *et al.*, J. High Energy Phys. 01 (2001) 010; HERWIG v6.504.
- [20] D. Acosta *et al.* (CDF Collaboration), Phys. Rev. Lett. **94**, 041803 (2005).
- [21] U. Baur and E. L. Berger, Phys. Rev. D **47**, 4889 (1993).